frontiers | Frontiers in Electronics

TYPE Original Research
PUBLISHED 18 February 2025
DOI 10.3389/felec.2025.1553891

Check for updates

OPEN ACCESS

EDITED BY
Qiao Peng,
Sichuan University, China

REVIEWED BY
Jing Lyu,
Shanghai Jiao Tong University, China
Xin Xiang,
Zhejiang University, China

*CORRESPONDENCE
Maolan Peng,
pml1081170912@163.com

RECEIVED 31 December 2024
ACCEPTED 27 January 2025
PUBLISHED 18 February 2025

CITATION
Peng M, He X, Xiao J, Feng L, Liao F and Jiang W (2025) Active short-circuit capacity identification method for LCC-HVDC system considering the integration of renewable energy.
Front. Electron. 6:1553891.
doi: 10.3389/felec.2025.1553891

COPYRIGHT
© 2025 Peng, He, Xiao, Feng, Liao and Jiang. This is an open-access article distributed under the terms of the Creative Commons Attribution License (CC BY). The use, distribution or reproduction in other forums is permitted, provided the original author(s) and the copyright owner(s) are credited and that the original publication in this journal is cited, in accordance with accepted academic practice. No use, distribution or reproduction is permitted which does not comply with these terms.

Active short-circuit capacity identification method for LCC-HVDC system considering the integration of renewable energy

Maolan Peng[1]*, Xiaopeng He[2], Jiachen Xiao[2], Lei Feng[1], Fangqun Liao[1] and Wen Jiang[2]

[1]Electric Power Research Institute, CSG EHV Power Transmission Company, Guangzhou, China, [2]State Key Laboratory of Alternate Electrical Power System with Renewable Energy Sources, North China Electric Power University, Beijing, China

For LCC-HVDC system with renewable energy integration, the randomness and variability of renewable energy will cause wide variations in the short-circuit capacity provided by the AC system. To effectively assess the supporting capability of the AC system, this paper proposes an active short-circuit capacity identification method for LCC-HVDC system considering the integration of renewable energy. First, an equivalent AC system was established based on Thevenin theorem, and the equivalent electromotive force was calculated. Then, the sensitivity of the voltage at the point of common coupling (PCC) to the active and reactive power flowing through the PCC was computed. Through sensitivity analysis, the key factors affecting the identification of the equivalent resistance and reactance were studied. Based on this, an active short-circuit capacity identification method combining the switching of filters and changes in DC power was proposed. Finally, a simulation model of LCC-HVDC system with grid-following wind power integration was built in PSCAD/EMTDC for verification. The results show that the proposed method is applicable to AC systems with different impedance characteristics. Moreover, with the increase of the grid-following renewable energy, the short-circuit capacity provided by the AC system shows a decreasing trend. The proposed method can actively identify the short-circuit capacity of AC system with renewable energy, thus provides a theoretical basis for the development of control strategies for LCC converter station under different AC system strength.

KEYWORDS

short-circuit capacity, active identification, LCC-HVDC system, renewable energy, Thevenin equivalent

1 Introduction

With the advancement of the green and low-carbon transformation in the power industry, renewable energy sources such as wind and photovoltaic power have been rapidly developed (Shu et al., 2021). The Line Commutated Converter based High Voltage Direct Current (LCC-HVDC) system, with its advantages in long-distance and large-capacity power transmission, has become a key transmission channel for the efficient consumption and utilization of renewable energy (Liu et al., 2014). For LCC-HVDC system with renewable energy integration, the short-circuit capacity provided by the AC grid at the converter bus is a critical indicator of system stability and a key basis for adjusting the control parameters and strategies of the DC converter station (Zhang and Kang, 2022). However, the large-scale replacement of traditional synchronous generators by renewable energy weakens the strength of the AC grid. Additionally, the intermittent and random characteristics of renewable energy cause the short-circuit capacity provided by the AC grid to fluctuate significantly, presenting challenges to the stable operation of the LCC-HVDC system (Hong et al., 2021). Therefore, accurately and quickly identifying the short-circuit capacity of LCC-HVDC systems with large-scale renewable energy integration is essential.

Many valuable studies have been conducted on active short-circuit capacity identification methods. which can generally be classified into two main technical approaches.

The first approach is the bus short-circuit testing method. Reference (Ma et al., 2017; Sun, 2018) propose conducting multiple artificial short-circuit experiments on AC and DC lines of LCC-HVDC projects to obtain short-circuit currents. Although this method ensures the accuracy of experimental data, it disrupts the normal operation of the grid and introduces safety risks. Reference (Sun et al., 2012) adds system topology analysis to the grid monitoring software, and then calculates the short-circuit capacity at each bus in the grid based on the grid model and traditional calculation methods. However, this approach relies on the premise that the grid monitoring system has comprehensive coverage.

The second method is the Thevenin equivalent impedance calculation method. Reference (Chu and Teng, 2021; Sanjay et al., 2022) combines traditional detection with machine learning to obtain the system Thevenin equivalent parameters by solving a nonlinear regression problem. However, in practice, the available real-time information is extremely limited, which cannot provide enough training samples, and the engineering application of artificial intelligence algorithms requires further development. Some studies have used the injection of non-characteristic harmonic currents into the AC grid to derive the Thevenin equivalent. Reference (Asiminoaei et al., 2005; Petrella et al., 2009) propose injecting harmonic currents of non-characteristic frequencies into the AC grid through the inverter's inner control loop, calculating the equivalent impedance of the AC grid at the injected harmonic frequencies, and then identifying the fundamental frequency equivalent impedance. The AC grid is then modeled as a Thevenin equivalent circuit to calculate its short-circuit capacity. On this basis, reference (Wu et al., 2021) addresses the difficulty of phase angle identification in weak grids by proposing a dual-harmonic injection impedance identification method, which reduces the Total Harmonic Distortion (THD) of the grid-connected inverter current. Reference (Yang et al., 2018) focuses on scenarios where specific background harmonic components dominate the grid voltage and proposes a method for detecting grid impedance using a modular complex filter with non-characteristic subharmonic injection.

Some literature also performs the Thevenin equivalent of the AC grid by applying active/reactive power disturbances. Reference (Ciobotaru et al., 2007; Choi et al., 2010) propose applying active and reactive power disturbances to the inverter control loop, measuring voltage and current magnitudes and phases at the common AC bus before and after the disturbances to calculate the AC grid's equivalent impedance. Reference (Li et al., 2022) proposes an active disturbance injection-based impedance measurement method. This method requires a high signal-to-noise ratio, and large disturbance signals are detrimental to the normal operation of the system under test. Reference (Ye et al., 2022) applies active and reactive power disturbances to the AC grid separately, using node voltage equations and Ohm's law to decompose the grid into active and reactive power balance circuits, improving the accuracy of the grid's equivalent impedance and short-circuit capacity identification. Reference (Abdi et al., 2022) demonstrates that under the conditions of rapid phase measurement technology, real-time tracking of system parameters can be achieved using local measurement information from multiple time instances, which provides an important reference for real-time monitoring of voltage support. Based on this, reference (Yu et al., 2024) focuses on renewable energy multi-infeed systems, and proposes an algorithmic flow covering system parameter identification, real-time index calculation and safety warning analysis, which can be used to evaluate the real-time voltage support. Reference (Hao et al., 2023) focuses on the MMC-HVDC system, proposing an online identification method for the equivalent impedance of the AC grid based on reactive power disturbance injection. Reference (Pan et al., 2023) focuses on the LCC-HVDC system, where short-circuit capacity is calculated by measuring the changes in the electrical quantities at the converter bus before and after switching the filter. However, the above methods do not account for the changes in the impedance characteristics of the AC system after the large-scale integration of renewable energy. In summary, in the study of short-circuit capacity identification, the artificial short-circuit test method can directly obtain short-circuit current but poses safety risks. Most Thevenin parameter identification methods are focused on AC grids or renewable energy stations and have not yet been applied to LCC-HVDC system with renewable energy integration. Therefore, it is necessary to propose an active short-circuit capacity identification method for LCC-HVDC system considering the impact of renewable energy integration.

The rest of the paper is organized as below. The Section 2 introduces the model of LCC-HVDC system with renewable energy integration, performing Thevenin equivalent of the AC system and analyzing the characteristics of short-circuit capacity variation. In Section 3, the expression for the equivalent system's source electromotive force is derived. Based on this, the sensitivity of the PCC (Point of Common Coupling) voltage to the active and reactive power flowing through the PCC is calculated. Sensitivity analysis identifies the key factors affecting the identification of the equivalent resistance and reactance parameters. Building on this, an active short-circuit capacity identification method is proposed, which combines filter switching with DC power variation. In Section 4, a simulation model of a LCC-HVDC system with grid-following renewable energy at the sending end is built in PSCAD/EMTDC for validation. The results show that the proposed method is applicable

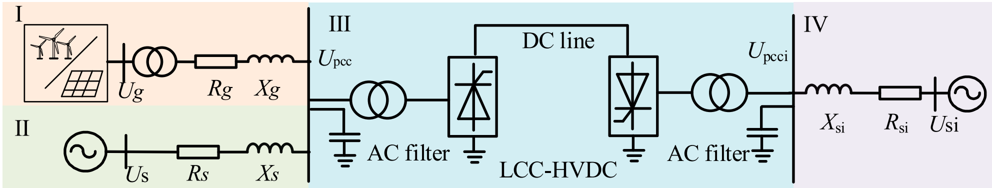

FIGURE 1
Schematic diagram of the LCC-HVDC system with renewable energy integration.

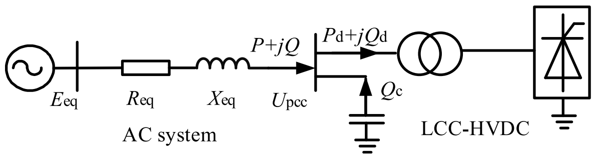

FIGURE 2
Equivalent analysis model of the sending-end AC system.

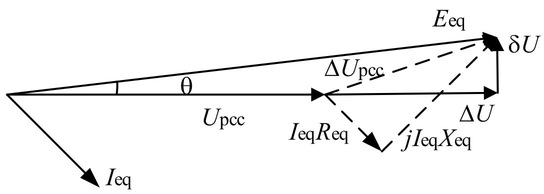

FIGURE 3
Phasor diagram of the voltage variation in the equivalent AC system.

to AC systems with different impedance characteristics, and that as the output of the grid-following renewable energy increases, the short-circuit capacity provided by the AC system shows a decreasing trend. Section 5 concludes the paper.

2 The model of LCC-HVDC system with renewable energy integration and short-circuit capacity analysis

2.1 System structure

Taking the case of renewable energy located at the sending-end AC system, the schematic diagram of the LCC-HVDC system with renewable energy integration is shown in Figure 1.

As shown in Figure 1, the system mainly consists of the renewable energy source (Region Ⅰ), traditional synchronous power source (Region Ⅱ and Ⅳ), and LCC-HVDC system (Region Ⅲ). Here, U_g is the voltage at the renewable energy station output, and R_g and X_g are the equivalent resistance and reactance of the renewable energy branch, respectively; U_s is the rectifier-side traditional AC source electromotive force, and R_s and X_s are the resistance and reactance of the traditional power source line; U_{si}, R_{si} and X_{si} are the electromotive force and impedance parameters of the inverter-side traditional AC source. U_{pcc} is the RMS voltage at the Point of Common Coupling (PCC), where renewable energy is integrated into the grid. To analyze the short-circuit capacity provided by the AC system, the rectifier-side AC system can be equivalently modeled, as shown in Figure 2.

2.2 Short-circuit capacity analysis

The short-circuit capacity of the LCC-HVDC system refers to the apparent power at the converter bus during a three-phase short circuit, which is the product of the rated voltage at the converter bus and the short-circuit current provided by the AC system to the converter bus, as shown in Equation 1. The larger the short-circuit capacity, the stronger the voltage support capability of the AC system and the better the voltage stability at the PCC point.

$$S_{ac} = \frac{E_{eq}U_N}{Z_{eq}} \tag{1}$$

Where E_{eq} is the electromotive force of the equivalent AC system; U_N is the rated voltage at the converter bus and Z_{eq} is the impedance of the equivalent AC system.

As shown in Figure 1, taking the rectifier side as an example, when no renewable energy is integrated, the short-circuit current at the converter bus is entirely provided by the traditional synchronous power source (Region Ⅰ). In this case, the short-circuit capacity is mainly related to the terminal voltage U_s of the traditional synchronous power source and the line impedance R_s,X_s . The higher the terminal voltage and the lower the line impedance, the greater the short-circuit capacity that the AC system can provide. However, when renewable energy is integrated into the AC system, the short-circuit current is provided jointly by both renewable energy and the traditional synchronous power source. The composition type of renewable energy, control strategy, grid connection method, and the output ratio between renewable energy and traditional power sources all influence the variation characteristics of short-circuit current, which in turn affects the short-circuit capacity of the LCC-HVDC system. Therefore, it is necessary to propose an active identification method for short-circuit capacity that takes the impact of renewable energy into account, in order to analyze the change of AC system strength after the integration of renewable energy.

3 Active identification method for short-circuit capacity of LCC-HVDC system with renewable energy integration

3.1 Principle of active identification of short-circuit capacity for LCC-HVDC system with renewable energy integration

From the above analysis, it can be seen that by obtaining the electromotive force and impedance parameters of the equivalent AC system, the short-circuit capacity at the PCC can be calculated using Equation 1.

Based on the equivalent analysis model of the system shown in Figure 2, we can obtain:

$$E_{eq} = U_{pcc} + I_{eq}\left(R_{eq} + jX_{eq}\right) \tag{2}$$

In Equation 2, I_{eq} is the current flowing into the PCC from the equivalent AC system.

The power injected into the PCC by the equivalent AC system can be given by Equation 3:

$$S = P + jQ = U_{pcc}\left(I_{eq}\right)^{*} \tag{3}$$

Taking the PCC point voltage as the reference phasor, by combining Equations 2, 3, the equivalent electromotive force is obtained as follows in Equation 4:

$$\begin{aligned} E_{eq} &= U_{pcc} + \frac{PR_{eq} + QX_{eq}}{U_{pcc}} + j\frac{PX_{eq} - QR_{eq}}{U_{pcc}} \\ &= U_{pcc} + \Delta U + j\delta U \end{aligned} \tag{4}$$

Where ΔU is the longitudinal component of the voltage drop, and δU is the transverse component of the voltage drop. The phasor diagram is shown in Figure 3:

Simplifying Equation 4 gives:

$$E_{eq} = \sqrt{\left(U_{pcc} + \frac{PR_{eq} + QX_{eq}}{U_{pcc}}\right)^2 + \left(\frac{PX_{eq} - QR_{eq}}{U_{pcc}}\right)^2} \tag{5}$$

The traditional short-circuit ratio identification method typically assumes that at high voltage levels, the line impedance angle is large, and the line resistance can be neglected. It is approximately considered that the line impedance $Z \approx X_{eq}$. In this case, Equation 5 can be simplified as:

$$E_{eq} = \sqrt{\left(U_{pcc} + \frac{QX_{eq}}{U_{pcc}}\right)^2 + \left(\frac{PX_{eq}}{U_{pcc}}\right)^2} \tag{6}$$

In Equation 6, the unknowns are E_{eq} and X_{eq}. The traditional method changes the system operating conditions by switching the filter, obtaining two sets of U_{pcc}, P and Q (namely, U_{pcc1}, P_1, Q_1 and U_{pcc2}, P_2, Q_2 before and after the filter switching), then substituting them into Equation 6 to solve for the equivalent parameters. The expression is as follows:

$$\begin{cases} E_{eq} = \sqrt{\left(U_{pcc1} + \dfrac{Q_1 X_{eq}}{U_{pcc1}}\right)^2 + \left(\dfrac{P_1 X_{eq}}{U_{pcc1}}\right)^2} \\ E_{eq} = \sqrt{\left(U_{pcc2} + \dfrac{Q_2 X_{eq}}{U_{pcc2}}\right)^2 + \left(\dfrac{P_2 X_{eq}}{U_{pcc2}}\right)^2} \end{cases} \tag{7}$$

Where the subscripts 1 and 2 represent the measured electrical quantities at the PCC under different operating conditions.

However, for LCC-HVDC system with renewable energy integration, first, the different grid connection methods of renewable energy can affect their electrical characteristics. For example, Grid-following (GFL) control is typically equivalent to a current source, while Grid-forming (GFM) control is typically equivalent to a voltage source. Additionally, the transmission lines from the renewable energy station to the converter bus usually include multiple segments of low-voltage level lines, where the line impedance angle is small, and the resistance component cannot be ignored. Therefore, the impedance characteristics of the equivalent AC system with renewable energy integration are not well-defined, and ignoring the line resistance may lead to inaccurate identification results. As a result, it is necessary to propose a short-circuit capacity identification method that simultaneously considers both the resistance and reactance characteristics.

Without neglecting the resistance, and assuming that the equivalent electromotive force and impedance of the AC system remain unchanged, Equation 5 contains three constant unknowns: E_{eq}、 R_{eq} and X_{eq}. Therefore, it is necessary to change the system operating conditions to obtain three sets of U_{pcc} as well as the active and reactive power flowing through the PCC. By combining these, E_{eq}、 R_{eq} and X_{eq} can be solved, as shown in the following equation:

$$\begin{cases} E_{eq} = \sqrt{\left(U_{pcc1} + \dfrac{P_1 R_{eq} + Q_1 X_{eq}}{U_{pcc1}}\right)^2 + \left(\dfrac{P_1 X_{eq} - Q_1 R_{eq}}{U_{pcc1}}\right)^2} \\ E_{eq} = \sqrt{\left(U_{pcc2} + \dfrac{P_2 R_{eq} + Q_2 X_{eq}}{U_{pcc2}}\right)^2 + \left(\dfrac{P_2 X_{eq} - Q_2 R_{eq}}{U_{pcc2}}\right)^2} \\ E_{eq} = \sqrt{\left(U_{pcc3} + \dfrac{P_3 R_{eq} + Q_3 X_{eq}}{U_{pcc3}}\right)^2 + \left(\dfrac{P_3 X_{eq} - Q_3 R_{eq}}{U_{pcc3}}\right)^2} \end{cases} \tag{8}$$

3.2 Active identification method for short-circuit capacity of LCC-HVDC systems with renewable energy integration

The following analyzes how to set the system operating conditions to obtain valid operating parameters. First, it is approximated that the phase angle of the equivalent electromotive force is close to that of the PCC voltage, and δU is neglected. Equation 4 can then be simplified in Equation 9:

$$E_{eq} \approx U_{pcc} + \frac{PR_{eq} + QX_{eq}}{U_{pcc}} \tag{9}$$

The sensitivity of the PCC point voltage to active and reactive power can be solved as follows:

$$\begin{cases} \dfrac{\partial U_{pcc}}{\partial P} = -\dfrac{R_{eq}}{2U_{pcc} - E_{eq}} \\ \dfrac{\partial U_{pcc}}{\partial Q} = -\dfrac{X_{eq}}{2U_{pcc} - E_{eq}} \end{cases} \tag{10}$$

Let the denominator of Equation 10 be approximated as $U_{pcc} \approx U_N$. Sensitivity analysis shows that, aside from the electromotive force E_{eq}, when the active power P injected at the PCC changes, the voltage variation at the PCC is mainly related to the equivalent resistance R_{eq}. Conversely, when the reactive power Q at the PCC changes, the voltage variation at the point is primarily influenced by the equivalent reactance X_{eq}. If multiple active power disturbances are applied to obtain electrical parameters under different operating conditions, the identification of the reactance parameters will be biased due to the insensitivity of the reactance to active power variations. Similarly, applying multiple reactive power disturbances will lead to bias in the resistance identification results due to the insensitivity of the resistance to reactive power variations. Therefore, to accurately identify the equivalent resistance and reactance parameters, both the active power and reactive power injected at the PCC point must be changed simultaneously. After obtaining the corresponding electrical parameters, E_{eq}、R_{eq} and X_{eq} can be effectively identified.

According to Figure 2, ignoring the active power injected by the AC filter into the converter bus, the power coupling relationship at the PCC is as follows:

$$\begin{cases} P = P_d \\ Q = Q_d + Q_c \end{cases} \tag{11}$$

Where P_d is the active power transmitted by the LCC-HVDC system, Q_d is the reactive power consumed by the converter station, and Q_c is the reactive power compensated by the filter.

As seen from Equation 11, changing the active power P_d transmitted by the HVDC system can cause a change in the active power P injected into the converter bus by the AC system. The reactive power Q injected into the converter bus by the AC system is related to the reactive power consumed by the converter station Q_d and the reactive power compensated by the filter Q_c. In LCC-HVDC system, there is a coupling between P_d and Q_d, so when the active power changes, the reactive power consumed will also change. However, since the active power transmitted by the LCC-HVDC system cannot be significantly reduced during online identification, the variation in reactive power caused by changing P_d is small. Therefore, in this study, the reactive power compensation Q_c injected into the converter bus is modified by disconnecting the filter, leading to a change in the reactive power supplied to the converter bus by the AC system.

As previously analyzed, both active power and reactive power changes need to be coordinated to achieve accurate identification of the resistance and reactance parameters. Based on this, this paper proposes an active identification method for the short-circuit capacity of LCC-HVDC system with the integration of renewable energy. The main process is outlined as follows, and the schematic diagram is shown in Figure 4, with flow chart shown in Figure 5.

(i) Step 1: Measure the RMS voltage at the PCC U_{pcc1} under rated operating conditions, along with the active power P_1 and reactive power Q_1 injected into the point by the AC system at this time.
(ii) Step 2: Disconnect a set of filters at the converter station to induce a change in the reactive power compensation. Measure the RMS voltage at the PCC U_{pcc2}, as well as the active power P_2 and reactive power Q_2 injected into the point by the AC system at this time.
(iii) Step 3: Change the DC power of the LCC-HVDC system using step current or power command values. After the system stabilizes, measure the electrical quantities U_{pcc3}, P_3, and Q_3.
(iv) Step 4: Substitute the measurements from steps (i) to (iii) into (8) and solve for the equivalent AC system's electromotive force E_{eq} and impedance parameters R_{eq} and X_{eq} .
(v) Step 5: Calculate the short-circuit capacity using Equation 1.

4 Validation by simulation studies

To verify the validity of the proposed active identification method for short-circuit capacity, a 500kV/1500 MW LCC-HVDC system with renewable integration at the sending end is constructed in PSCAD/EMTDC. The rectifier side uses constant-current control, while the inverter side employs constant-voltage control. The system structure is shown in Figure 6:

The sending end includes traditional synchronous generators and wind turbines, with the wind turbines operating under Grid-following (GFL) control. The AC filter bank is equipped with dual-tuned filters (Type A), triple-tuned filters (Type B), and single-tuned filters (Type C), with a configuration of 2A+2B+1C. Other system parameters are provided in Table 1.

4.1 The verification of the active short-circuit capacity identification method for LCC-HVDC

Based on Figure 4, the proposed short-circuit capacity identification method requires the application of both active and reactive disturbances. The reactive disturbance is introduced by disconnecting the filters, while the active disturbance can be achieved by changing the current reference value or power reference value. Considering that the rectifier side of the LCC-HVDC system used in this paper operates under constant current control, the following approach combines filter disconnection with a step change in the current reference value to alter the PCC voltage and injected power.

Figure 7 shows the electrical quantities of the LCC-HVDC system (i.e., U_{pcc}, P and Q) for different operating conditions obtained using the method proposed in this paper.

As shown in Figure 7, operating condition I represents the rated operating condition. At time t_1, one set of AC filters is disconnected, resulting in operating condition II. At time t_2, the reference current is stepped from 1pu to 0.95pu, which defines operating condition III. By substituting the electrical quantities under these three operating conditions into Equation 8, the system's short-circuit capacity can be determined.

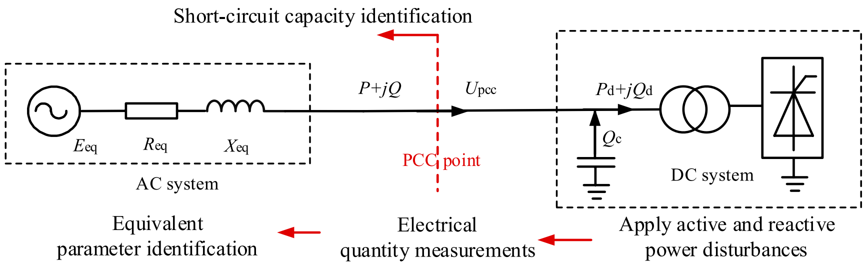

FIGURE 4
Schematic diagram of short-circuit capacity identification.

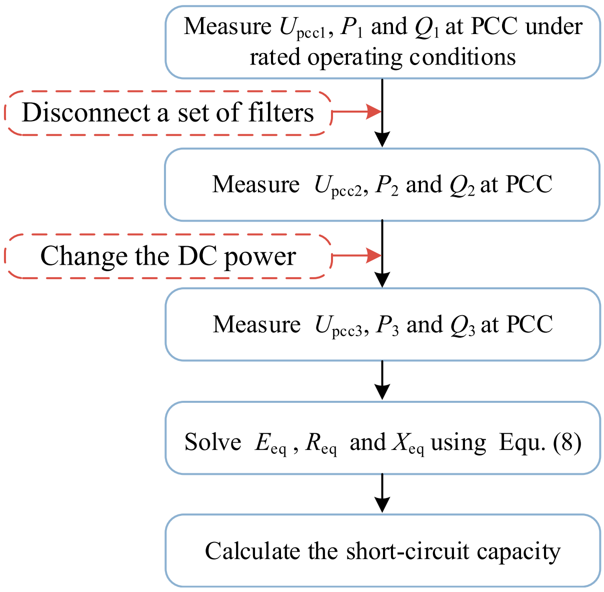

FIGURE 5
Flow chart of short-circuit capacity identification method.

TABLE 1 Main parameters of the system.

Voltage level	Parameters	Values
35 kV	Transformer ratio, leakage reactance	0.69 kV/35 kV, 0.1pu
	Unit resistance	0.0621 Ω/km
	Unit inductance	0.00036 H/km
	Unit capacitance	0.21 uF/km
	Line length	2 km
525 kV	Transformer ratio, leakage reactance	35 kV/525 kV, 0.15 pu
	Unit resistance	0.01808 Ω/km
	Unit inductance	0.00088 H/km
	Line length	50 km

To verify the applicability of the proposed method to AC systems with different impedance characteristics, the renewable energy output is first set to zero. In this case, the sending-end AC system consists solely of traditional synchronous generators. The system's equivalent impedance is then the equivalent impedance of the synchronous generator, and the system's electromotive force is the electromotive force of the traditional power source.

Set the equivalent impedance of the traditional power source as Z_N = 36.75Ω. By varying the impedance angle of the traditional power source, different scenarios for changes in the resistive component are simulated. Meanwhile, the power source's electromotive force is adjusted to maintain the PCC voltage at the rated AC voltage.

The following two cases are set up to identify the short circuit capacity at different impedances:

Case A: The traditional method proposed in reference (Pan et al., 2023), which neglects the resistance, obtains two sets of electrical quantities under two operating conditions (i.e., the rated condition 1 and condition 2 after filter disconnection, as shown in Figure 7). These quantities are substituted into Equation 7 to solve for E_{eq} and X_{eq}.

Case B: The method proposed in this paper, which considers the resistive component, obtains three sets of electrical quantities under three operating conditions (i.e., the rated condition 1, condition 2 after filter disconnection, and condition 3 obtained by changing the current reference value, as shown in Figure 7). These quantities are substituted into Equation 8 to calculate E_{eq}, R_{eq}, and X_{eq}.

Tables 2, 3 present the identification results of the source electromotive force and impedance for the equivalent AC system, respectively.

From the above tables, it can be concluded that the short-circuit capacity active identification method considering resistive component proposed in this paper, which combines filter switching and DC power variation, provides high accuracy in identifying the equivalent electromotive force and impedance parameters of the AC system under different impedance angles. In contrast, as the impedance angle increases, the accuracy of the method that neglects the resistance decreases. This demonstrates the

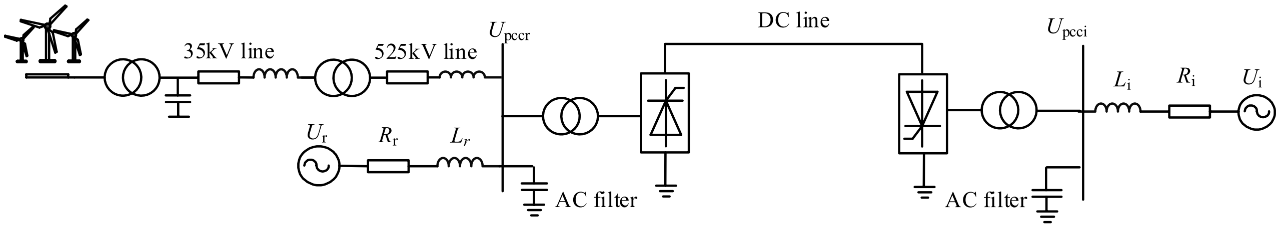

FIGURE 6
The LCC-HVDC system with new energy access.

TABLE 2 The results of equivalent impedance Z_{eq}.

Impedance angle/°	Case A		Case B	
	Zeq/Ω	Error	Zeq/Ω	Error
0	1.32	96.43%	36.93	0.49%
10	8.04	78.03%	36.60	0.39%
20	14.35	60.85%	36.66	0.25%
30	19.94	45.91%	36.87	0.31%
40	25.06	32.04%	36.87	0.35%
50	29.33	20.38%	36.84	0.25%
60	32.9	11.50%	37.18	1.15%
70	35.15	4.98%	36.99	0.66%
80	37.06	1.01%	37.44	1.88%
90	37.38	0.03%	37.39	1.74%

TABLE 3 The results of equivalent electromotive force E_{eq}.

Impedance angle/°	E_s/ kV	Case A		Case B	
		E/kV	Error	E/kV	Error
0	629.13	525.23	16.59%	629.71	0.09%
10	628.97	525.23	16.43%	628.50	0.07%
20	626.17	529.65	15.34%	625.63	0.09%
30	620.78	532.27	14.26%	620.81	0.00%
40	612.89	535.11	12.67%	612.72	0.03%
50	602.66	537.76	10.68%	602.04	0.10%
60	590.28	540.2	8.50%	590.39	0.02%
70	576.00	541.83	5.82%	575.31	0.12%
80	560.15	543.32	2.79%	558.92	0.22%
90	543.06	543.56	0.44%	541.18	0.35%

applicability of the proposed method to AC systems with varying impedance characteristics.

4.2 The verification of the active short-circuit capacity identification method for LCC-HVDC

For LCC-HVDC transmission systems with renewable energy integration on the AC side, the voltage level at the renewable energy station's grid connection is relatively low. Multiple voltage step-ups are required from the station's output to the grid connection point, resulting in several low-voltage lines in the renewable energy branch. In this case, the resistive component of the lines cannot be neglected.

Based on the above analysis, the method proposed in this paper demonstrates good applicability under different impedance characteristics of the AC system. Therefore, based on the method proposed in this paper, the impedance characteristics can be considered for identifying the equivalent parameters of the AC system with renewable energy integration, thereby obtaining a more accurate short-circuit capacity.

Currently, renewable energy stations are predominantly located in remote areas where the grid infrastructure is often underdeveloped. This results in a weak connection between the renewable energy stations and the AC grid, leading to scenarios where renewable energy is integrated into a weak AC network. Therefore, when identifying the short-circuit capacity of LCC-HVDC with renewable energy integration, it is essential to investigate how the short-circuit capacity varies under different levels of AC system strength.

Assume the equivalent impedance of the traditional synchronous generator is Z_s. The strength of the traditional AC power source is typically described by the short-circuit ratio, denoted as SCR_{tra}, which is expressed in Equation 12:

$$SCR_{tra} = \frac{U_N^2}{Z_s P_{dN}} = \frac{1}{Z_{s\_pu}} \tag{12}$$

where U_N represents the rated voltage of the converter bus, and P_{dN} is the rated transmission power of the DC system. Taking U_N and P_{dN} as the base voltage and capacity, Z_{s_pu} represents the per-unit value of the equivalent impedance.

For the test model shown in Figure 6, the strength of the traditional AC power source is adjusted, and the short-circuit capacity provided to the converter bus by the equivalent AC system is identified and analyzed for renewable energy output shares of 0pu, 0.4pu, 0.5pu, and 0.6pu. The identification results are shown in Tables 4–6 below.

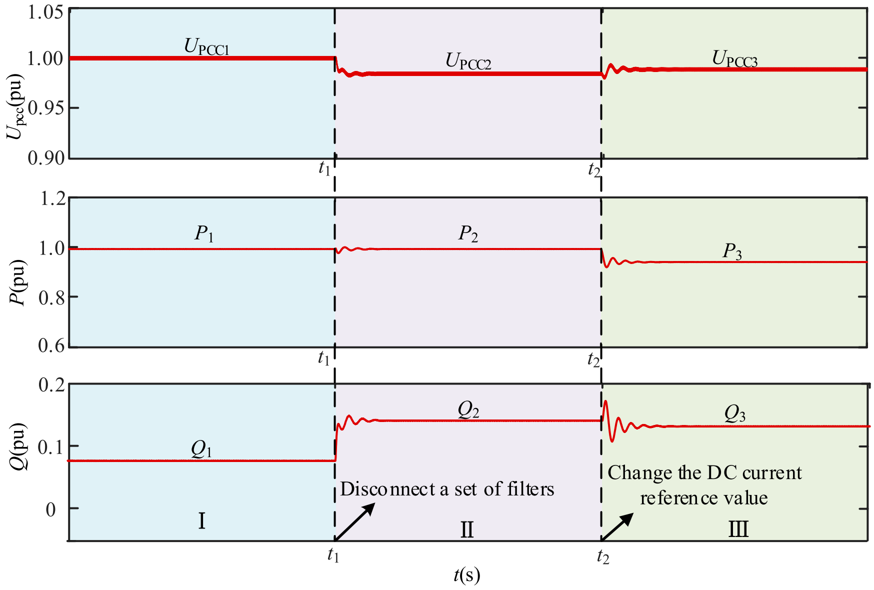

FIGURE 7
The electrical quantities for different operating conditions.

TABLE 4 The short-circuit capacity identification results when SCR_{tra} = 5.

Renewable energy output/pu	E_S/kV	R_{eq}/Ω	X_{eq}/Ω	Z_{eq}/Ω	Impedance angle/°	S_{ac}/MVA
0	558.1	1.73	37.96	38.00	87.39	7710.71
0.4	547.65	−1.24	39.63	39.65	91.79	7251.47
0.5	540.25	−2.17	40.72	40.78	93.05	6955.53
0.6	528.69	−4.29	44.59	44.80	95.50	6196.15

TABLE 5 The short-circuit capacity identification results when SCR_{tra} = 3.

Renewable energy output/pu	E_S/kV	R_{eq}/Ω	X_{eq}/Ω	Z_{eq}/Ω	Impedance angle/°	S_{ac}/MVA
0	583.34	3.43	61.54	61.64	86.81	4968.78
0.4	563.2	−5.78	64.97	65.23	95.08	4533.12
0.5	548.31	−10.28	69.4	70.16	98.43	4103.11
0.6	519.9	−20.98	80.08	82.78	104.68	3297.16

Case 1: The impedance of the traditional AC power source is set to Z_{s_pu} = 0.2pu, i.e., SCR_{tra} = 5.
Case 2: The impedance of the traditional AC power source is set to Z_{s_pu}≈0.33pu, i.e., SCR_{tra} = 3.
Case 3: The impedance of the traditional AC power source is set to Z_{s_pu} = 0.5pu, i.e., SCR_{tra} = 2.

From the comparison of Tables 4–6, the following observations can be made:

1) As the share of renewable energy output increases, the impedance angle of the equivalent AC system shows a decreasing trend, while the proportion of the equivalent resistance component continues to rise. Moreover, this trend becomes more pronounced as the strength of the traditional AC power source decreases. Therefore, when identifying the short-circuit capacity of LCC-HVDC with renewable energy integration, the resistive component cannot be neglected, which also validates the applicability of the short-circuit capacity identification method proposed in this paper in new energy access scenarios.
2) The short-circuit capacity that the equivalent AC system can provide varies significantly with changes in renewable energy

TABLE 6 The short-circuit capacity identification results when SCR_{tra} = 2.

Renewable energy output/pu	E_S/kV	R_{eq}/Ω	X_{eq}/Ω	Z_{eq}/Ω	Impedance angle/°	S_{ac}/MVA
0	618.16	5.6	91.79	91.96	86.51	3529.05
0.4	581.17	−15.8	95.09	96.39	99.43	3165.29
0.5	551.86	−28.74	102.24	106.20	105.7	2728.05
0.6	The DC transmission system cannot operate stably					

output: as the proportion of Grid-following (GFL) renewable energy output increases, the equivalent electromotive force of the AC system gradually decreases, and the system's equivalent impedance continues to increase, which means that the short-circuit capacity at the DC system's converter bus is greatly reduced. In this case, the traditional short-circuit ratio is no longer an effective indicator of the equivalent AC system's strength. Furthermore, when the strength of the traditional AC power source is weak, a high proportion of renewable energy output may cause the system to fail to operate stably.

5 Conclusion

In this paper, an active identification method for short-circuit capacity in LCC-HVDC with renewable energy integration is proposed, which combines filter switching and DC power variation and can provide theoretical guidance for the development of control strategies for LCC-HVDC transmission systems. The main conclusions are as follows:

1) The proposed short-circuit capacity identification method, which combines filter switching and DC power variation, can accurately identify the equivalent impedance and electromotive force of the equivalent AC system, thereby determining the equivalent short-circuit capacity. This method is also applicable to AC systems with different impedance characteristics.
2) For LCC-HVDC system with renewable energy integration, as the proportion of renewable energy output increases, the impedance angle of the equivalent AC system decreases, and the proportion of the equivalent resistance component increases. Moreover, this trend becomes more pronounced as the strength of the traditional AC power source weakens. Therefore, when performing online identification of the system's short-circuit capacity, the equivalent resistance cannot be neglected.
3) In LCC-HVDC system with renewable energy integration, as the proportion of renewable energy output gradually increases, the equivalent electromotive force of the AC system decreases, the equivalent impedance increases, and the system's equivalent short-circuit capacity shows a downward trend. The weakening of the AC system strength makes traditional short-circuit ratio indicators ineffective for assessing the system strength. Additionally, an excessively high renewable energy output may lead to system instability.

Data availability statement

The original contributions presented in the study are included in the article/supplementary material, further inquiries can be directed to the corresponding author.

Author contributions

MP: Writing–original draft. XH: Writing–original draft. JX: Writing–original draft. LF: Writing–review and editing. FL: Writing–review and editing. WJ: Writing–review and editing.

Funding

The author(s) declare that financial support was received for the research, authorship, and/or publication of this article. This work is supported by the Science and Technology Project of China Southern Power Grid EHV Power Transmission Company, China Southern Power Grid Joint Laboratory of DC transmission Equipment and Submarine Cable Safety Operation (Research on Identification of Short Circuit Capacity and Stability Control Technology of HVDC System, No. 0120002023030301SJ00078).

Conflict of interest

Authors MP, LF, and FL were employed by CSG EHV Power Transmission Company.

The remaining authors declare that the research was conducted in the absence of any commercial or financial relationships that could be construed as a potential conflict of interest.

The authors declare that this study received funding from China Southern Power Grid EHV Power Transmission Company. The funder had the following involvement in the study: study design.

Generative AI statement

The author(s) declare that no Generative AI was used in the creation of this manuscript.

Publisher's note

All claims expressed in this article are solely those of the authors and do not necessarily represent those of their affiliated organizations, or those of the publisher, the editors and the reviewers. Any product that may be evaluated in this article, or claim that may be made by its manufacturer, is not guaranteed or endorsed by the publisher.

References

Abdi, P., Hamedani-Golshan, M.-E., Alhelou, H., and Milano, F. (2022). A PMU-based method for on-line Thévenin equivalent estimation. *IEEE Trans. Power Syst.* 37 (4), 2796–2807. doi:10.1109/tpwrs.2021.3125007

Asiminoaei, L., Teodorescu, R., Blaabjerg, F., and Borup, U. (2005). A digital controlled PV-inverter with grid impedance estimation for ENS detection. *IEEE Trans. Power Electron.* 20 (6), 1480–1490. doi:10.1109/tpel.2005.857506

Choi, D., Kang, D., and Lee, K. (2010). "A novel gain scheduling method for distributed power generation systems with a LCL-filter by estimating grid impedance," in *2010 IEEE international symposium on industrial electronics*. Bari, Italy, 3438–3443.

Chu, Z., and Teng, F. (2021). Short circuit current constrained UC in high IBG-penetrated power systems. *IEEE Trans. Power Syst.* 36 (4), 3776–3785. doi:10.1109/tpwrs.2021.3053074

Ciobotaru, M., Teodorescu, R., and Rodriguez, P. (2007). "Online grid impedance estimation for single-phase grid-connected systems using PQ variations," in *2007 IEEE power electronics specialists conference*. Orlando, USA, 2306–2312.

Hao, X., Guo, C., and Jiang, W. (2023). Identification method for equivalent impedance of AC power grid connected to MMC-HVDC system based on reactive power injection. *Automation Electr. Power Syst.* 47 (9), 184–192.

Hong, Q. T., Khan, M. A. U., Henderson, C., Egea-Àlvarez, A., Tzelepis, D., and Booth, C. (2021). Addressing frequency control challenges in future low-inertia power systems: a great Britain perspective. *Engineering* 7 (8), 1057–1063. doi:10.1016/j.eng.2021.06.005

Li, M., Nian, H., and Hu, B. (2022). Review of perturbation signals applied to impedance measurement of renewable generator. *Proc. CSEE* 42 (17), 6296–6316. doi:10.13334/j.0258-8013.pcsee.211467

Liu, Z., Zhang, Q., and Dong, C. (2014). Efficient and security transmission of wind, photovoltaic and thermal power of large-scale energy resource bases through UHVDC projects. *Proc. CSEE* 34 (16), 2513–2522. doi:10.13334/j.0258-8013.pcsee.2014.16.001

Ma, Y., Huang, C., and Wang, K. (2017). Measurement and frequency analysis of short current and its ground wire shunting at artificial grounding fault on AC and DC transmission lines. *High. Volt. Eng.* 43 (12), 3914–3921. doi:10.13336/j.1003-6520.hve.20171127013

Pan, W., Lu, D., Cui, H., and Lu, Y. (2023). Real time detection method for operation short circuit ratio of ultra high voltage direct current system and its application in control systems. *Electr. Eng.* 24 (9), 71–75+79.

Petrella, R., Revelant, A., and Stocco, P. (2009). "Advances on inter-harmonic variable-frequency injection-based grid-impedance estimation methods suitable for PV inverters," in *2009 IEEE energy conversion congress and exposition*, 1173–1179.

Sanjay, K., Barjeev, T., Vishal, K., and Sunita, C. (2022). PMU-based voltage stability measurement under contingency using ANN. *IEEE Trans. Instrum. Meas.* 71, 1–11. doi:10.1109/tim.2021.3129210

Shu, Y., Zhang, L., Zhang, Y., Wang, Y., Lu, G., Yuan, B., et al. (2021). Carbon peak and carbon neutrality path for China's power industry. *Strategic Study CAE* 23 (6), 1–14. doi:10.15302/j-sscae-2021.06.001

Sun, Y. (2018). *Research on fast detection technology of short circuit current in electrical power system. [master's thesis]. [Harbin (China)]*. Harbin University of Science and Technology.

Sun, Y., Xu, J., and Huang, L. (2012). A short-circuit capacity online monitoring method and device based on dynamic transfer impedance. Pat. CN102707161A.

Wu, X., Liang, J., Tong, Y., and Tang, F. (2021). Research on method of grid impedance estimation by complex filters based initiative harmonic injection. *Power Syst. Technol.* 37 (10), 2796–2801. doi:10.13335/j.1000-3673.pst.2013.10.045

Yang, Y., Zhang, X., and Li, M. (2018). Grid impedance detection method under unbalanced and harmonic grid voltage based on multiple complex coefficient filters. *J. Power Supply* 16 (02), 69–75. doi:10.13234/j.issn.2095-2805.2018.2.69

Ye, P., Han, X., and Yu, Y. (2022). P-Q disturbance decoupled Thevenin equivalent for power grids. *Proc. CSEE* 42 (9), 3239–3250. doi:10.13334/j.0258-8013.pcsee.210261

Yu, L., Sun, H., and Xu, S. (2024). Research on the real-time measurement method of the strength of the power system with high penetration of renewable energies. *Proc. CSEE.* doi:10.13334/j.0258-801

Zhang, Z., and Kang, C. (2022). Challenges and prospects for constructing the new-type power system towards a carbon neutrality future. *Proc. CSEE* 42 (08), 2806–2819. doi:10.13334/j.0258-8013.pcsee.220467